A Reassessment of the First Metal-Carbonyl Dissociation Energy in $M(CO)_4$ (M = Ni, Pd, Pt), $M(CO)_5$ (M = Fe, Ru, Os), and $M(CO)_6$ (M = Cr, Mo, W) by a Quasirelativistic Density Functional Method

Jian Li, Georg Schreckenbach, and Tom Ziegler*

Contribution from the Department of Chemistry, University of Calgary, Calgary, Alberta, Canada T2N 1N4

Received April 18, 1994[⊗]

Abstract: A nonlocal, quasirelativistic density functional (DF) method, NL-SCF+QR, has been applied to the calculation of M-CO bond lengths and the first bond dissociation energy (FBDE) in the binary transition metal carbonyls $M(CO)_4$ (M = Ni, Pd, Pd), $M(CO)_5$ (M = Fe, Ru, Os), and $M(CO)_6$ (M = Cr, Mo, W). The calculated M-CO bond lengths are in good agreement with available experimental data with an error typically smaller than 0.01 Å. The calculated FBDE's are 29.9 (Ni), 12.3 (Pd), 15.7 (Pt), 45.7 (Fe), 33.0 (Ru), 34.7 (Os), 46.2 (Cr), 39.7 (Mo), and 43.7 (W) kcal/mol, respectively. These values compare well with the available experimental estimates of 25 (Ni), 42 (Fe), 28 (Ru), 31 (Os), 37 (Cr), 41 (Mo), and 46 (W), respectively. Calculations have also been carried out on the CO association energy, AE, corresponding to the following process: $M(CO)_6 + CO$ (M = Cr, Mo, W) $\rightarrow M(CO)_7 + AE$. The calculated AE's are 47.0 (Cr), 40.4 (Mo), and 35.8 (W) kcal/mol. These calculations underline that CO substitution in $M(CO)_6$ (M = Cr, Mo, W) can proceed by CO dissociation as well as CO association. The relativistic effects are found to contract M-CO bonds by between 0.07 and 0.16 Å and strengthen the FBDE's by 5-11 kcal/mol for third-row compounds. The relativistic stabilization of the FBDE's among the 5d elements makes in general the M-CO bond of the 4d element the weakest within a triad. The way in which relativity enhances the M-CO bond is analyzed by an energy decomposition scheme based on the Extended Transition State (ETS) method.

I. Introduction

Many important organometallic reactions are initiated by the thermal or photolytic dissociation of a CO ligand from a coordinatively saturated metal complex. It is therefore understandable that a considerable effort has been devoted to studies on the thermal stability and kinetic lability of the metal-carbonyl bond.[1] Unfortunately, an accurate measurement of the first M-CO bond dissociation energy (FBDE) is difficult even for simple transition metal carbonyls. The few available experimental data on FBDE's of binary transition metal carbonyls have been determined by techniques based on kinetics, photoacoustic calorimetry,[2,3] or pulsed laser pyrolysis.[4] However, the experimental data obtained so far are too limited to provide a clear picture of how FBDE's change with the metal center and the nature of the ancillary ligands. Also, the lack of experimental information makes it difficult to estimate reaction enthalpies in which metal-carbonyl bond making and bond breaking is involved.

Theoretically, FBDE's can be calculated successfully[26] by highly correlated *ab initio* methods such as the coupled cluster scheme (CCSD(T))[5] or the modified coupled-pair functional (MCPF)[6] method. However, the calculations are rather expensive especially for molecules containing second- or third-row transition metals or complexes with low symmetry.

Density functional theory (DFT), on the other hand, has proven to be a powerful tool in studies of transition metal compounds.[7] Tschinke[8] *et al.* have previously published a DFT based study on the FBDE's of the metal carbonyls $M(CO)_4$ (M = Ni, Pd, Pt), $M(CO)_5$ (M = Fe, Ru, Os), and $M(CO)_6$ (M = Cr, Mo, W).[8] In this investigation, all calculations were based on experimental or assumed structures due to the lack of efficient geometry optimization methods at the time. Also, the calculations were carried out with a simple DFT scheme in which Becke's[9] nonlocal (NL) corrections were treated as a perturbation to the energy expression based on the local density approximation (LDA),[10,11] whereas nonlocal corrections to correlation were neglected.

Great strides have been made in DFT theory[7,12] and methodology[7,12b] since the FBDE calculations by Tschinke[8] et al. It is now possible to optimize molecular geometries,[13]

[⊗] Abstract published in *Advance ACS Abstracts*, December 15, 1994.

(1) (a) Marks, T. J. *Bonding energetics in organometallic compounds*; ACS Symposium Series 248; American Chemical Society: Washington, DC, 1990. (b) Simoes, J. A. M.; Beauchamp, J. L. *Chem. Rev.* **1990**, *90*, 629.

(2) (a) Angelici, R. J. *Organomet. Chem. Rev. A3* **1968**, 173. (b) Covey, W. D.; Brown, T. L. *Inorg. Chem.* **1973**, *12*, 2820. (c) Centinis, G.; Gambino, O. *Atti Accad. Sci. Torino I* **1963**, *97*, 1197. (d) Werner, H. *Angew. Chem., Int. Ed. Engl.* **1968**, *7*, 930. (e) Graham, J. R.; Angelici, R. J. *Inorg. Chem.* **1967**, *6*, 2082. (f) Werner, H.; Prinz, R. *Chem. Ber.* **1960**, *99*, 3582. (g) Werner, H.; Prinz, R. *J. Organomet. Chem.* **1966**, *5*, 79.

(3) Bernstein, M.; Smith, J. D.; Peters, G. D. *Chem. Phys. Lett.* **1983**, *100*, 241.

(4) Lewis, K. E.; Golden, D. M.; Smith, G. P. *J. Am. Chem. Soc.* **1984**, *106*, 3905.

(5) Raghavachari, K.; Trucks, G. W.; Pople, J. A.; Head-Gordon, M. *Chem. Phys. Lett.* **1989**, *157*, 479.

(6) Chong, D. P.; Langhoff, S. R. *J. Chem. Phys.* **1986**, *84*, 5606.

(7) Ziegler, T. *Chem. Rev.* **1991**, *91*, 651.

(8) Ziegler, T.; Tschinke, V.; Ursenbach, C. *J. Am. Chem. Soc.* **1987**, *109*, 4825.

(9) Becke, A. *J. Chem. Phys.* **1986**, *84*, 4524.

(10) Stoll, H.; Golka, E.; Preuss, H. *Theor. Chim. Acta* **1980**, *55*, 29.

(11) Vosko, S. J.; Wilk, L.; Nusair, M. *Can. J. Phys.* **1980**, *58*, 1200.

(12) (a) Parr, R. G.; Yang, W. *Density Functional Theory of Atoms and Molecules*; Oxford University Press: New York, 1988. (b) Labanowski, J.; Andzelm, J. *Density Functional Methods in Chemistry*; Springer-Verlag: Heidelberg, 1991.

(13) (a) Versluis, L.; Ziegler, T. *J. Chem. Phys.* **1988**, *88*, 322. (b) Fan, L.; Ziegler, T. *J. Chem. Phys.* **1991**, *95*, 7401.

0002-7863/95/1517-0486$09.00/0

evaluate vibrational frequencies[14] and intensities,[14b,c] optimize transition state structures,[15a,b] and trace reaction paths.[15c−e] Heavy metal complexes can in addition be treated by fully self-consistent relativistic methods[16] with complete geometry optimization. Progress has in addition been made with the development of new and powerful nonlocal functionals,[17] and these have been implemented self-consistently.[14d]

We have in previous studies applied the new DFT methodology to metal−carbon,[18] metal−hydrogen,[18] and metal−metal[18] σ-bond energies. The present investigation will make use of the same DFT techniques in a reassessment of FBDE's for binary metal carbonyls.

II. Computational Details

The calculations reported here were carried out by using the density functional package, ADF, developed by Baerends *et al.*[19a] and vectorized by Ravenek.[19b] The adopted numerical integration scheme was that developed by te Velde *et al.*[20] A set of uncontracted triple-ζ Slater-type orbitals (STO) was employed for the ns, np, nd, $(n+1)$s, and $(n+1)$p valence orbitals of the transition metal atoms.[21] For the 2s and 2p orbitals of carbon and oxygen, use was made of a double-ζ basis augmented by an extra 3d polarization function.[21] The inner-core shells were treated by the frozen-core approximation.[19] A set of auxiliary s, p, d, f, and g STO functions, centered on all nuclei, was introduced to fit the molecular density and to present Coulomb and exchange potentials accurately.[22] All molecular geometries were optimized according to the analytic energy gradient method implemented by Verslius and Ziegler at the LDA level[13a] and by Fan and Ziegler at the nonlocal (NL) level, NL-SCF.[13b] The NL corrections adopted were based on Becke's functional for exchange[9,17b] and Perdew's functional for correlation.[17a]

The relativistic effects were taken into account at two levels of theory. In the lower level scheme based on first-order perturbation theory (FO),[23] terms up to first order in α^2 (α is the fine structure constant) are retained in the Hamiltonian as a perturbation, and therefore, the energy of the molecule includes contributions from the mass-velocity, Darwin, and spin−orbit terms. In the more elaborate quasirelativistic method (QR),[24] changes in the density induced by the first-order Hamiltonian are taken into account to all orders of α^2 whereas operators in the Hamiltonian to second and higher orders are neglected. The QR scheme can readily be extended to include energy gradients of importance for structure optimizations.[16] Recently, van Lenthe et al. developed a new relativistic regular two-component Hamiltonian (denoted as CPD),[25] which incorporates relativistic effects to high accuracy. To examine the validity of the FO and QR methods, we have compared the FBDE for $Pt(CO)_4$ calculated by the FO and QR schemes with the FBDE for $Pt(CO)_4$ obtained by van Lenthe[25b] et al. using the CPD method.[25a] The calculations were all based on the NL-SCF+QR geometry. The calculated FBDE's are 16.7 (FO), 15.7 (QR), and 15.5 kcal/mol (CPD). It would thus appear that the FO and QR schemes, especially the latter, can treat relativistic effects with a high degree of accuracy.

The first bond dissociation energy (FBDE) of $M(CO)_n$ corresponds to the reaction enthalpy of the process

$$M(CO)_n \rightarrow M(CO)_{n-1} + CO \qquad (1)$$

The DFT calculated values reported in this work represent the electronic contribution to the reaction enthalpy of eq 1. No vibrational zero-point energy (ZPE) and thermal correction are included. However, it can be estimated that these two corrections, roughly, tend to cancel each other and that the net correction is rather small. For example, the net correction is estimated to be 0.5, 0.1, and 0.2 kcal/mol, respectively, for $Cr(CO)_6$, $Mo(CO)_6$, and $W(CO)_6$, based on Hartree−Fock frequency calculations.[26]

We have analyzed the different factors of importance for the M−CO bond by decomposing the FBDE's with the help of the extended transition state (ETS)[27] method as

$$-\mathrm{FBDE} = E_{\mathrm{steric}} + E_{\mathrm{orb}} + E_{\mathrm{prep}} \qquad (2a)$$

Here E_{steric} represents the steric interaction energy between the fragments CO and $M(CO)_{n-1}$. This term is made up of the (stabilizing) electrostatic interaction between the two fragments as well as the repulsive destabilizing two-orbital-four-electron interactions between occupied orbitals on the two fragments. The term E_{orb} originates from stabilizing interactions between occupied and virtual orbitals of the two separate fragments. This term can be divided further into contributions from different symmetry representations (Γ) of the molecular point group preserved during formation of $M(CO)_n$ from CO and $M(CO)_{n-1}$ according to[8,27b]

$$E_{\mathrm{orb}} = \sum_{\Gamma} E_{\mathrm{orb}}^{\Gamma} \qquad (2b)$$

The contributions to E_{orb} from the CO to metal donation can be distinguished from the contribution due to the CO to metal back-donation in those cases where the two-charge-transfer process involves orbitals belonging to different symmetry representations.[8,27b] The last term, E_{prep}, comes from the energy required to relax the structures of the free fragments to the geometries they take up in the combined $M(CO)_n$ complex. A more detailed description of the ETS scheme and its applications to metal carbonyls can be found elsewhere.[8,27]

III. Results and Discussion

a. Saturated $M(CO)_4$ (M = Ni, Pd, Pt) Species. Among the tetracarbonyl compounds of the platinum triad, $Ni(CO)_4$ is the only one stable at room temperature whereas $Pd(CO)_4$ and $Pt(CO)_4$ have been characterized only in low-temperature matrices.[28] We have optimized the geometries of the coordinatively saturated d^{10} tetracarbonyls $M(CO)_4$ (M = Ni, Pd, and Pt) within tetrahedral T_d symmetry constraints. The M−C and

(14) (a) Fan, L.; Versluis, L.; Ziegler, T.; Baerends, E. J.; Ravenek, W. *Int. J. Quantum Chem.* **1988**, *S22*, 173. (b) Fan, L.; Ziegler, T. *J. Chem. Phys.* **1992**, *96*, 9005. (c) Fan, L.; Ziegler, T. *J. Phys. Chem.* **1992**, *96*, 6937. (d) Fan, L.; Ziegler, T. *J. Phys. Chem.* **1991**, *94*, 6057.

(15) (a) Fan, L.; Ziegler, T. *J. Chem. Phys.* **1990**, *92*, 3645. (b) Fan, L.; Ziegler, T. *J. Am. Chem. Soc.* **1992**, *114*, 10890. (c) Deng, L.; Fan, L.; Ziegler, T. *J. Chem. Phys.* **1993**, *99*, 3823. (d) Deng, L.; Ziegler, T. *Int. J. Quantum Chem.*, in press. (e) Deng, L.; Ziegler, T. *J. Am. Chem. Soc.* Submitted for publication.

(16) Schreckenbach, G.; Ziegler, T. Unpublished work.

(17) (a) Perdew, J. P. *Phys. Rev.* **1986**, *B33*, 8822; Erratum, *ibid* **1986**, *B34*, 7406. (b) Becke, A. *Phys. Rev.* **1988**, *A38*, 3098. (c) Lee, C.; Yang, W.; Parr, R. G. *Phys. Rev.* **1988**, *B37*, 785. (d) Perdew, J. P.; Wang, Y. *Phys. Rev.* **1992**, *B45*, 13244. (e) Wilson, L. C.; Levy, M. *Phys. Rev.* **1990**, *B41*, 12930.

(18) Folga, E.; Ziegler, T. *J. Am. Chem. Soc.* **1993**, *115*, 5170.

(19) (a) Baerends, E. J.; Ellis, D. E.; Ros, P. *Chem. Phys.* **1973**, *2*, 41. (b) Ravenek, W. In *Algorithms and applications on vector and parallel computers*; te Riele, H. J. J., Dekker, Th. J., van de Vorst, H. A.; Eds.; Elsevier: Amsterdam, 1987.

(20) (a) Boerrigter, P. M.; te Velde, G.; Baerends, E. J. *Int. J. Quantum Chem.* **1988**, *33*, 87. (b) te Velde, G.; Baerends, E. J. *J. Comput. Phys.* **1992**, *99*, 84.

(21) (a) Snijders, J. G.; Baerends, E. J.; Vernooijs, P. *At. Nucl. Data Tables* **1982**, *26*, 483. (b) Vernooijs, P.; Snijders, J. G.; Baerends, E. J. *Slater type basis functions for the whole periodic system*; Internal report, Free University of Amsterdam, The Netherlands, 1981.

(22) Krijn, J.; Baerends, E. J. *Fit functions in the HFS-method*; Internal report (in Dutch), Free University of Amsterdam, The Netherlands, 1984.

(23) (a) Snijders, J. G.; Baerends, E. J. *Mol. Phys.* **1978**, *36*, 1789. (b) Snijders, J. G.; Baerends, E. J.; Ros, P. *Mol. Phys.* **1979**, *38*, 1909.

(24) Ziegler, T.; Tschinke, V.; Baerends, E. J.; Snijders, J. G.; Ravenek, W. *J. Phys. Chem.* **1989**, *93*, 3050.

(25) (a) van Lenthe, E.; Baerends, E. J.; Snijders, J. G.; Ravenek, W. *J. Chem. Phys.* **1993**, *99*, 4597. (b) van Lenthe, E. Private communication.

(26) (a) Ehlers, A. W.; Frenking, G. *J. Chem. Soc., Chem. Commun.* **1993**, 1709. (b) Ehlers, A. W.; Frenking, G. *J. Am. Chem. Soc.* **1994**, *116*, 1514.

(27) (a) Ziegler, T.; Rauk, A. *Theor. Chim. Acta* **1977**, *46*, 1. (b) Ziegler, T. *NATO ASI* **1986**, *C176*, 189. (c) Baerends, E. J.; Rozendaal, A. *NATO ASI* **1986**, *C176*, 159. (d) Ziegler, T. *NATO ASI* **1992**, *C378*, 367.

(28) Kundig, E. P.; McIntosh, D.; Moskovits, M.; Ozin, G. A. *J. Am. Chem. Soc.* **1973**, *95*, 7234.

Table 1. M−CO and C−O Bond Lengths (Å) in $M(CO)_4$ and $M(CO)_3$

	$Ni(CO)_4$		$Pd(CO)_4$		$Pt(CO)_4$	
method	M−C	C−O	M−C	C−O	M−C	C−O
LDA	1.779	1.140	1.985	1.139	2.050	1.138
NL-SCF	1.830	1.150	2.086	1.148	2.176	1.144
NL-SCF+QR	1.829	1.150	2.056	1.147	2.012	1.151
MP2[a]	1.873	1.181	2.032	1.178	2.100	1.178
MCPF[b]	1.883	1.167				
CCSD(T)[c]	1.831					
exp[d]	1.838	1.141				
	$Ni(CO)_3$		$Pd(CO)_3$		$Pt(CO)_3$	
method	M−C	C−O	M−C	C−O	M−C	C−O
LDA	1.765	1.145	1.978	1.141	2.044	1.139
NL-SCF	1.829	1.153	2.053	1.147	2.134	1.146
NL-SCF+QR	1.827	1.150	1.993	1.148	1.997	1.150

[a] Reference 32. [b] Reference 31. [c] Reference 30. [d] Reference 29.

C−O bond lengths determined by DFT techniques as well as *ab initio* methods are collected in Table 1.

The geometry of $Ni(CO)_4$ has been used extensively as a test for theoretical methods since highly accurate experimental data are available.[29] The Ni−CO bond length calculated at the LDA level is too short, by 0.06 Å, compared to experiment. The agreement between the experimental and calculated Ni−CO bond length is improved considerably by including nonlocal corrections, NL-SCF. The deviation is now less than 0.01 Å, an accuracy only matched by the highly correlated and computationally demanding CCSD(T)[30,31] scheme. The less accurate MP2 *ab initio* scheme is seen to overestimate the Ni−CO distance by 0.035 Å. Also the CO distance with R(C−O) = 1.181 Å was found to be much longer than the experimental estimate of 1.141 Å. The NL-SCF bond length is by comparison 1.150 Å, Table 1.

The nonlocal NL-SCF scheme in which relativity is neglected finds the Pd−CO bond distance of 2.086 Å to be shorter than the Pt−CO bond length of 2.176 Å. However, this order is reversed after the inclusion of relativity in the NL-SCF-QR calculation. Now R(Pd−CO) = 2.056 Å and R(Pt−CO) = 2.012 Å. Thus, relativity has contracted the Pt−CO distance by a full 0.164 Å to the point where it becomes shorter than the Pd−CO distance for which the relativistic contraction only amounts to 0.024 Å. The best *ab initio* calculations on $Pd(CO)_4$ and $Pt(CO)_4$ were carried out at the MP2 level[32] with the aid of relativistic effective core potentials (RECP); no comparable nonrelativistic *ab initio* calculations were available to assess the influence of relativity. The MP2 calculations find the Pt−CO bond at 2.100 Å to be longer than the Pd−CO distance at 2.03 Å. Thus, the MP2 method does not predict the 5d element to have the shortest M−CO bond. It would be interesting to extend the higher level CCSD(T) calculations to the 4d and 5d elements.

Experimental estimates of the M−CO bond distances in $M(CO)_4$ (M = Pd, Pt) are not available. The only known experimental Pt−CO bond lengths are 1.86 Å in $Pt(PPh_3)_3CO$ and 1.92 Å in $Pt(PPh_2Et)(CO)_2$.[33] However, these distances are likely to be shorter than in $Pt(CO)_4$, where four, rather than one, π-acceptor ligands are competing for electron density from the same metal center.

Table 2. First Bond Dissociation Energies (kcal/mol) for $M(CO)_4$

method[a]	$Ni(CO)_4$	$Pd(CO)_4$	$Pt(CO)_4$
LDA	44.9	25.9	20.4
LDA/NL	28.9	11.1	6.0
LDA/NL+FO	30.7	16.0	14.7
NL-SCF	28.7	10.9	3.4
NL-SCF/FO	30.5	13.5	13.2
NL-SCF+QR	29.9	12.3	15.7
MCPF[b]	24.0		
CCSD(T)[c]	29.8		
exp[d]	25 ± 2		

[a] LDA/NL+FO means that the geometry is optimized at the LDA level and the nonlocal (NL) and relativistic corrections (FO) are treated as perturbations. For NL-SCF/FO the nonlocal (NL) corrections are treated self-consistently whereas the relativistic corrections (FO) are added as perturbation. NL-SCF-QR treat nonlocal and relativistic corrections fully self-consistent. [b] Reference 31. [c] Reference 30. [d] Reference 35.

Methods based on matrix IR spectroscopy have identified the coordinatively unsaturated d^{10} complexes $Ni(CO)_3$ and $Pd(CO)_3$ and deduced that they most likely possess a trigonal planar D_{3h} geometry.[34] A DFT geometry optimization carried out within C_{3v} symmetry constraints converged to the planar D_{3h} conformation for all three species $M(CO)_3$ (M = Ni, Pd, and Pt). The calculated bond distances are collected in Table 1. No experimental data or structures optimized by *ab initio* methods are available. The M−CO bond distances are in general shorter in the $M(CO)_3$ species than in the $M(CO)_4$ complexes as fewer CO ligands compete for electron density from the same metal center in the former species. We note again the large relativistic effect on the Pt−CO distance and the more modest contraction of the Pd−CO bond.

The FBDE's for the tetracarbonyls of Ni, Pd, and Pt are shown in Table 2, together with experimental[35] data and other theoretical estimates[30,31] for $Ni(CO)_4$. It follows from Table 2 that our NL-SCF+QR value for $Ni(CO)_4$ is in excellent agreement with the CCSD(T) result but about 5 kcal/mol larger than the experimental estimate. No experimental data are available for $Pd(CO)_4$ and $Pt(CO)_4$. The FBDE's calculated by DFT are relatively small, only half the value of the FBDE for $Ni(CO)_4$. This is in accordance with the fact that the 4d and 5d homologues are rather unstable compared to $Ni(CO)_4$.

Relativity has as large an impact on the strength of the Pt−CO bond as it had on its length. We have included relativity at a lower level as a perturbation (FO) and at a higher level (QR) in a fully self-consistent manner. Either of the schemes afford a substantial stabilization of the Pt−CO bond of between 10 (FO) and 12.5 (QR) kcal/mol. The corresponding stabilization of the Pd−CO bond is around 2 kcal/mol. Relativity has the interesting effect of making the Pt−CO bond shorter and stronger than its Pd−CO counterpart, Tables 1 and 2.

Lack of experimental data for the Pd−CO and Pt−CO bond makes it impossible to confirm our predicted order of Ni ≫ Pt > Pd for the bond strengths. However, it is interesting to note that the 4d palladium member in the homologous series $M[P(OEt)_3]_4$ (M = Ni, Pd, Pt) is the substitutionally most labile.[46]

b. Unsaturated $M(CO)_4$ (M = Fe, Ru, Os) Species. The calculation of the FBDE's for the saturated d^8 pentacarbonyls

(29) Hedberg, L.; Ijima, T.; Hedberg, K. *J. Chem. Phys.* **1979**, *70*, 3224.
(30) Blomberg, M. R. A.; Siegbahn, P. E. M.; Lee, T. J.; Rendell, A. P.; Rice, J. E. *J. Chem. Phys.* **1991**, *95*, 5898.
(31) (a) Blomberg, M. R. A.; Brandemark, U. B.; Siegbahn, P. E. M.; Wennerberg, J.; Bauschlicher, C. W., Jr. *J. Am. Chem. Soc.* **1988**, *110*, 6650. (b) Bauschlicher, C. W., Jr.; Langhoff, S. R. *Chem. Phys.* **1989**, *129*, 431.
(32) Rohlfing, C. M.; Hay, P. J. *J. Chem. Phys.* **1985**, *83*, 4641.
(33) (a) Albano, V. G.; Ricci, G. M. R.; Bellon, P. L. *Inorg. Chem.* **1969**, *8*, 2109. (b) Albano, V. G.; Bellon, P. L.; Manassero, M. *J. Organomet. Chem.* **1972**, *35*, 423.
(34) (a) DeKock, R. L. *Inorg. Chem.* **1971**, *10*, 1205. (b) Kundig, E. P.; Moskovits, M.; Ozin, G. A. *Can. J. Chem.* **1972**, *50*, 3587.
(35) Stevens, A. E.; Feigerle, C. S.; Lineberger, W. C. *J. Am. Chem. Soc.* **1982**, *104*, 5026.

Table 3. Optimized Geometries for the Coordinatively Unsaturated M(CO)$_4$ Species[a]

	LDA		NL-SCF		NL-SCF+QR	MCPF[b]	
	$^3B_2$	$^1A_1$	$^3B_2$	$^1A_1$	$^1A_1$	$^3B_2$	$^1A_1$
Fe(CO)$_4$							
M−C$_{ax}$	1.800	1.775	1.859	1.834	1.831	1.879	1.910
M−C$_{eq}$	1.756	1.746	1.820	1.793	1.789	1.885	1.875
C−O$_{ax}$	1.147	1.146	1.156	1.153	1.153	1.169	1.181
C−O$_{eq}$	1.148	1.152	1.160	1.160	1.160	1.175	1.178
α(C$_{ax}$−M−C$_{ax}$)	154.6	177.0	147.4	167.7	165.9	150	151
β(C$_{eq}$−M−C$_{eq}$)	95.0	130.2	99.4	129.8	130.0	104	125
Ru(CO)$_4$							
M−C$_{ax}$	1.952	1.929		1.991	1.974		
M−C$_{eq}$	1.873	1.906		1.991	1.943		
C−O$_{ax}$	1.148	1.143		1.149	1.152		
C−O$_{eq}$	1.147	1.149		1.153	1.159		
α(C$_{ax}$−M−C$_{ax}$)	153.1	171.6		167.4	167.6		
β(C$_{eq}$−M−C$_{eq}$)	98.4	134.7		144.0	142.0		
Os(CO)$_4$							
M−C$_{ax}$	2.018	2.007		2.059	1.980		
M−C$_{eq}$	1.929	1.989		2.040	1.978		
C−O$_{ax}$	1.147	1.139		1.149	1.153		
C−O$_{eq}$	1.147	1.143		1.151	1.154		
α(C$_{ax}$−M−C$_{ax}$)	159.0	174.2		161.0	155.0		
β(C$_{eq}$−M−C$_{eq}$)	94.8	156.8		152.0	148.0		

[a] Bond lengths in angstroms and bond angles in degrees. [b] Reference 39.

Table 4. Calculated Singlet−Triplet Energy Splittings, E(S) − E(T) (kcal/mol)

method	Fe(CO)$_4$	Ru(CO)$_4$	Os(CO)$_4$
LDA	−4.0	−16.3	−22.0
LDA/NL+FO	1.7 (1.8)[a]	−13.1	−16.2
MCPF[b]	2.9		

[a] The data in parentheses are calculated at the NL-SCF+QR level. [b] Reference 39.

M(CO)$_5$ with M = Fe, Ru, and Os requires a knowledge of the molecular and electronic ground state structure for the unsaturated species M(CO)$_4$ (M = Fe, Ru, Os). However, what is the exact molecular and electronic ground state of M(CO)$_4$ is in itself an interesting question that has received considerable attention.[36,37] Experimental investigations based on kinetics, magnetic circular dichroism (MCD) and infrared spectroscopy (IR) seem to imply that Fe(CO)$_4$ possesses a triplet[36a] ground state whereas the lowest energy state for Ru(CO)$_4$ and Os(CO)$_4$ seems to be a singlet.[36f]

We have carried out geometry optimization studies on the M(CO)$_4$ (M = Fe, Ru, Os) species within C_{2v} symmetry constraints. Considerations were given to the $^1A_1$ singlet with a $(1a_2)^2(1b_1)^2(1a_1)^2(1b_2)^2$ configuration as well as the $^3B_2$ triplet with a $(1a_2)^2(1b_1)^2(1a_1)^2(1b_2)^1(2a_1)^1$ configuration.[37a] The optimized geometries and calculated singlet−triplet energy splittings are shown in Tables 3 and 4.

The optimized singlet geometries for M(CO)$_4$ possess a butterfly structure, **1**. The α(C$_{ax}$−M−C$_{ax}$) angle in **1** is close to 180°, and hence the singlet conformation can be regarded as having a trigonal bipyramidal structure in which one of the equatorial sites is vacant.[38] The optimized triplet structure resembles on the other hand a distorted tetrahedron, **2**, in which the α angle is close to 150°.

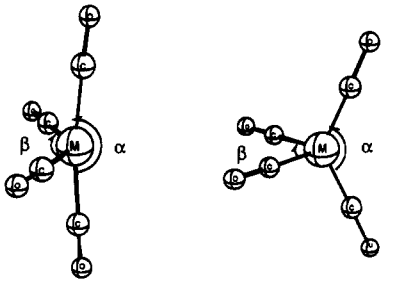

1 **2**

We find at the NL-SCF level the optimized ground state of Fe(CO)$_4$ to be a $^3B_2$ triplet with a distorted tetrahedral geometry, **2**, in which $\alpha = 148°$ and $\beta = 100°$. The $^1A_1$ singlet was found to be 1.8 kcal/mol higher in energy at the highest level of theory (NL-SCF+QR) with the butterfly conformation given by **1**, Tables 3 and 4. Our findings are in good agreement with experimental estimates.[36a] Thus, Poliakoff[36a] et al. found that Fe(CO)$_4$ has a triplet ground state based on MCD measurements and deduced in addition a distorted tetrahedral structure, **2**, with $\alpha = 150°$ and $\beta = 120°$ from IR intensity data. Lyne[37d] et al. have previously found a triplet ground state for Fe(CO)$_4$ in a DFT study where nonlocal corrections were neglected in the geometry optimization step but included in the energy calculations as a perturbation.

The most accurate *ab initio* calculations[37b,39] on Fe(CO)$_4$ are due to Barnes[39] *et al.* They found a $^3B_2$ triplet ground state for Fe(CO)$_4$ at the MCPF level of theory. Their optimized bond angles are quite similar to the NL-SCF estimates, whereas the Fe−CO distances are longer by 0.06−0.08 Å. The Fe−CO distances determined by the MCPF scheme for Fe(CO)$_5$ are, as we shall see later, too long by 0.03−0.06 Å compared to experiment, and it is thus likely that they are overestimated in the Fe(CO)$_4$ case as well. Barnes[39] et al. have also reported an approximate structure for the $^1A_1$ singlet state optimized by an uncoupled variation of each degree of freedom. Again, the optimized angular geometry is similar to ours whereas the Fe−CO bonds are longer by 0.08 Å. Based on the approximate geometry optimization for the $^1A_1$ state, the MCPF method afforded a splitting of 15 ± 5 kcal/mol.[39]

The two heavier congeners Ru(CO)$_4$ and Os(CO)$_4$ were both found to have a $^1A_1$ singlet ground state with a butterfly geometry, **1**. The corresponding $^3B_2$ triplet states are positioned 13−16 kcal/mol higher in energy, Table 4. Bogdan[36e,f] et al. have recently assigned a singlet ground state to Ru(CO)$_4$ and Os(CO)$_4$ based on measurements of the recombination rate for the process M(CO)$_4$ + CO → M(CO)$_5$. Bogdan[36e,f] et al. found that this rate is 10^3 times faster for M = Ru and Os than for M = Fe. They concluded that the rate is slower for iron since the recombination in that case is spin-forbidden with Fe(CO)$_4$ in a triplet state. By contrast, the singlet ground state of Ru(CO)$_4$ and Os(CO)$_4$ makes the recombination process involving these species spin-allowed and much faster.

The calculated singlet−triplet energy splittings, E(S) − E(T), are compiled in Table 4. We note that the simple LDA scheme incorrectly predicts Fe(CO)$_4$ to have a singlet ground state. The inclusion of nonlocal corrections as a perturbation, LDA/NL,

(36) (a) Poliakoff, M.; Weitz, E. *Acc. Chem. Res.* **1987**, *20*, 408. (b) Barton, T. J.; Grinter, R.; Thomson, A. J.; Davis, B.; Poliakoff, M. *J. Chem. Soc., Chem. Commun.* **1977**, 841. (c) Lionel, T.; Morton, J. R.; Preston, K. F. *J. Chem. Phys.* **1982**, *76*, 234. (d) Poliakoff, M.; Turner, J. J. *J. Chem. Soc., Dolton Trans.* **1974**, 2276. (e) Bogdan, P.; Weitz, E. *J. Am. Chem. Soc.* **1989**, *111*, 3163. (f) Bogdan, P.; Weitz, E. *J. Am. Chem. Soc.* **1990**, *112*, 639.

(37) (a) Elian, M.; Hoffmann, R. *Inorg. Chem.* **1975**, *14*, 1058. (b) Daniel, C.; Benard, M.; Dedieu, a.; Wiest, R.; Veillard, A. *J. Phys. Chem.* **1984**, *88*, 4805. (c) Ziegler, T.; Tschinke, V.; Fan, L.; Becke, A. D. *J. Am. Chem. Soc.* **1989**, *111*, 9177. (d) Lyne, P. D.; Mingos, D. M. P.; Ziegler, T.; Downs, A. J. *Inorg. Chem.* **1993**, *32*, 4785.

(38) Gillespie, R.; Hargittai, I. *VSEPR Theory of Molecular Geometry*; Allyn and Bacon: New York, 1990.

(39) Barnes, L. A.; Rosi, M.; Bauschlicher, C. W., Jr. *J. Chem. Phys.* **1991**, *94*, 2031.

Table 5. M−CO and C−O Bond Lengths (Å) of $M(CO)_5$

	$Fe(CO)_5$				$Ru(CO)_5$				$Os(CO)_5$			
method	$M-C_{ax}$	$M-C_{eq}$	$C-O_{ax}$	$C-O_{eq}$	$M-C_{ax}$	$M-C_{eq}$	$C-O_{ax}$	$C-O_{eq}$	$M-C_{ax}$	$M-C_{eq}$	$C-O_{ax}$	$C-O_{eq}$
LDA	1.769	1.789	1.145	1.149	1.934	1.931	1.142	1.147	2.003	1.988	1.140	1.147
NL-SCF	1.819	1.816	1.153	1.157	1.983	1.980	1.149	1.154	2.061	2.050	1.147	1.153
NL-SCF+QR	1.817	1.813	1.153	1.156	1.968	1.960	1.150	1.157	2.000	1.975	1.147	1.156
MRCI[a]	1.798	1.835										
MCPF[b]	1.878	1.847	1.168	1.177								
exp[c]	1.807	1.827	1.152	1.152	1.950[d]	1.969[d]	1.143	1.143	1.990[e]	1.943[e]	1.142	1.142

[a] Reference 41. [b] Reference 39. [c] $Fe(CO)_5$ from ref 41, $Ru(CO)_5$ from ref 42, $Os(CO)_5$ from ref 43. [d] Estimated errors are 0.01 Å for Ru−CO bonds. [e] Estimated errors are 0.02 Å for Os−CO bonds.

affords on the other hand the correct ground state for $Fe(CO)_4$. The singlet−triplet energy splitting for $Fe(CO)_4$ is not changed much further by a fully self-consistent nonlocal calculation, NL-SCF. Thus the splitting $E(S) - E(T)$ is calculated to be 1.7 and 1.8 kcal/mol by the LDA/NL and NL-SCF schemes, respectively.

There are at least two reasons why $Fe(CO)_4$ is high-spin whereas the heavier homologues are low spin. The first has to do with the fact that the d−d exchange interaction decreases down a triad as the *n*d orbitals become more diffuse, thus making spin-pairing less favorable. The second factor is related to the fact that the singly occupied $2a_1$ orbital of the triplet configuration **2** is strongly antibonding with respect to d_{z^2} on the metal and σ_{CO} orbitals on the ligands.[37a] This antibonding interaction is enhanced down the triad as the d-orbitals become more diffuse and overlap more strongly with the σ_{CO} orbitals. Thus, it becomes less favorable to occupy $2a_1$. It is a general phenomenon that the 3d member in a homologous series of compounds has a high-spin ground state whereas the 4d and 5d members are low-spin.

c. $M(CO)_5$ (M = Fe, Ru, Os). Experimental techniques based on X-ray and electron diffraction as well as IR spectroscopy have established that the d^8 pentacarbonyls of iron, ruthenium, and osmium all have a D_{3h} trigonal-bipyramidal structure.[40] We present in Table 5 optimized structures for the pentacarbonyls based on DFT calculations carried out within D_{3h} symmetry constraints. Accurate experimental[40a] data are available for all members of the $M(CO)_5$ family and they are included in Table 5 for comparison along with optimized structures for $Fe(CO)_5$ obtained by high-level *ab initio* techniques.[39,41]

The agreement between the Fe−CO distances determined by the NL-SCF+QR scheme and experimental estimates is excellent and nearly as good as the fit obtained by the multireference configuration-interaction (MRCI) method.[41] The Fe−CO and CO distances obtained by the MCPF scheme are on the other hand too long. We note again that the inclusion of nonlocal corrections in the geometry optimization, NL-SCF, results in a substantial improvement over the LDA structures, Table 5. The LDA metal−ligand bond distances are in general too short.

Hedberg[42,43] et al. have recently determined the structures of $Ru(CO)_5$ and $Os(CO)_5$ by gas-phase electron diffraction. Their observed distances[42] for $Ru(CO)_5$ of $Ru-CO_{eq} = 1.969$ Å and $Ru-CO_{ax} = 1.950$ Å are in good agreement with the NL-SCF+QR estimates given by $Ru-CO_{ax} = 1.968$ Å and $Ru-CO_{eq} = 1.960$ Å. The experimental values are associated with errors of 0.01 Å. We note that both nonlocal and relativistic corrections are important for a good agreement with experiment, although they cancel each other to some degree. Relativistic effects are seen to contract the Ru−CO bond by 0.02 Å. The experimental[43,44] bond distances for $Os(CO)_5$ are $Os-CO_{ax} = 1.990$ Å and $Os-CO_{eq} = 1.943$ Å, again in good agreement with the NL-SCF+QR estimates given by $Os-CO_{ax} = 2.000$ Å and $Os-CO_{eq} = 1.975$ Å. The error associated with the experimental estimates is 0.02 Å. We note that the Os−CO contraction due to relativity amounts to between 0.06 and 0.08 Å.

Table 6. The First Bond Dissociation Energies (kcal/mol) of $M(CO)_5$

method[a]	$Fe(CO)_5$	$Ru(CO)_5$	$Os(CO)_5$
LDA	65.9 (69.5)[b]	48.6	39.9
LDA/NL	46.1 (44.4)	30.1	22.4
LDA/NL+FO	47.1 (45.4)	35.0	36.0
NL-SCF	44.8 (43.0)	29.7	25.2
NL-SCF/FO	46.3 (44.5)	35.0	36.6
NL-SCF+QR	45.7 (43.9)	33.0	34.7
MCPF[c]	39 ± 5 (23.9)		
exp[d]	42		
exp[e]	40[e]	27.6[f]	30.6[f]

[a] See footnote *a* to Table 2. [b] Data in parentheses correspond to a spin-forbidden dissociation to triplet $Fe(CO)_4$ and CO. [c] Reference 39. [d] Accurate gas-phase value based on pulsed laser pyrolysis, ref 4. [e] Estimate based on solution kinetics, ref 45b. [f] Estimates based on solution kinetics, ref 45a.

Table 6 displays calculated and observed FBDE's for the pentacarbonyls. The accurate experimental gas-phase FBDE for $Fe(CO)_5$ of 42 kcal/mol was obtained by techniques based on pulsed laser pyrolysis,[4] and it is assumed to correspond to a dissociation of $Fe(CO)_5$ into singlet $Fe(CO)_4$ and CO. Basolo et al.[45b] have provided an estimate for the FBDE of 40 kcal/mol based on solution kinetics. We calculate a value of 45.7 kcal/mol for the dissociation of $Fe(CO)_5$ into singlet $Fe(CO)_4$ at the highest level of DFT theory, NL-SCF+QR. The corresponding spin-forbidden dissociation into triplet $Fe(CO)_4$ was determined by NL-SCF+QR to require 43.9 kcal/mol. Barnes[39] et al. determined a value of 24 kcal/mol for the triplet dissociation based on MCPF calculations and inferred in addition a singlet dissociation energy of 39 kcal/mol by adopting a value of 15 kcal for the $E(S) - E(T)$ separation in $Fe(CO)_4$ based on an approximate singlet structure. The $E(S) - E(T)$ separation by Barnes et al. is much larger than our estimate. It would be interesting to determine the $E(S) - E(T)$ separation in $Fe(CO)_4$ based on the CCSD(T) method with full geometry optimization.

Accurate gas-phase FDBE's are not available for $Ru(CO)_5$ and $Os(CO)_5$. However, the FBDE's of $Ru(CO)_5$ and $Os(CO)_5$ have been estimated by solution kinetics. Thus, Poe[45a] et al. and Basolo[45b] et al. studied the substitution reaction

(40) (a) Beagley, B.; Schmidling, D. G. *J. Mol. Struct.* **1974**, *22*, 466. (b) Calderazzo, F.; Eplattenier, L. *Inorg. Chem.* **1967**, *6*, 1220.

(41) Lüthi, H. P.; Siegbahn, P. E. M.; Almlöf, J. *J. Phys. Chem.* **1985**, *89*, 2156.

(42) Huang, J.; Hedberg, K.; Pomeroy, R. K. *Inorg. Chem.* **1990**, *29*, 3923.

(43) Huang, J.; Hedberg, K.; Pomeroy, R. K. *Organometallics* **1988**, *7*, 2049.

(44) Churchill, M. R.; Hollander, F. J.; Hutchinson, J. P. *Inorg. Chem.* **1977**, *16*, 2655.

(45) (a) Huq, R.; Poe, A. J.; Chawla, S. *Inorg. Chim. Acta* **1979**, *38*, 121. (b) Shen, J.-K.; Gao, Y.-C.; Shi, Q.-Z.; Basolo, F. *Inorg. Chem.* **1989**, *28*, 4304.

$$M(CO)_5 + L \rightarrow M(CO)_4L + CO \qquad M = Fe, Ru, Os \quad (3a)$$

and established that the rate-determining step involves CO dissociation

$$M(CO)_5 \rightarrow M(CO)_4 + CO \quad (3b)$$

By equating the observed activation energy, $\Delta H^{\#}$, for the substitution reaction of eq 3a with the bond dissociation energy of eq 3b they found the FBDE values 40, 27.6, and 30.6 kcal/mol for M = Fe, Ru, and Os, respectively. The kinetic data for M = Ru and Os compare reasonable well with the NL-SCF+QR estimates of 33.0 (Ru) and 34.7 (Os) kcal/mol. We note further that the calculated relativistic ordering for the FBDE's of these three compounds, $Fe(CO)_5 \gg Os(CO)_5 > Ru(CO)_5$, is in accordance with kinetic measurements,[45,46] which indicate that $Ru(CO)_5$ is thermally less stable and kinetically more labile than the iron and osmium congeners.

The interesting periodic trends within the iron triad are dictated by the fact that relativity contracts the Os−CO bond by 0.06 to 0.08 Å and strengthen it by 14 (FO) to 10 (QR) kcal/mol whereas the corresponding impact on the Ru−CO bond is smaller, although not negligible. We are not aware of any *ab initio* calculations on the structures and FBDE's of $Ru(CO)_5$ and $Os(CO)_5$.

d. $M(CO)_6$ and $M(CO)_7$ (M = Cr, Mo, W). Experimental data on the molecular structure and FBDE's of the group 6 hexacarbonyls are available for all members of the chromium triad. The experimental studies have further been supplemented by a number of theoretical investigations. Ehlers[26] and Frenking have most recently calculated the FBDE's for $M(CO)_6$ (M = Cr, Mo, W) by the highly accurate CCSD(T) method with the geometries determined by MP2. We have also determined the molecular structures and FBDE's for $M(CO)_6$ (M = Cr, Mo, W) by the NL-SCF-QR scheme.[47]

Table 7 compares the experimental[48] and calculated[26,47,49] geometries. It can be seen that both the MP2 scheme and the NL-SCF+QR method reproduce experimental geometries with very high accuracy: the error of the NL-SCF+QR method is less than 0.01 Å for M−C and C−O bond lengths. Estimates of the FBDE's based on CCSD(T) and NL-SCF+QR calculations are compared with experimental estimates in Table 8. It follows from Table 8 that the agreement between theory and experiment is excellent for $Mo(CO)_6$ and $W(CO)_6$. The situation is different for $Cr(CO)_6$ where the theoretical values of 46.2 (NL-SCF+QR) and 45.8 kcal/mol (CCSD(T)) are much larger than the best experimental estimate of 38.8 kcal/mol due to Lewis[4] et al. Ehlers[26] and Frenking attributed the deviation with experiment to errors in the MP2 geometries and obtained a FBDE value of 33 kcal/mol after adopting the experimental geometry for $Cr(CO)_6$ and an assumed structure for $Cr(CO)_5$. One might alternatively note that the gas-phase FBDE of $Cr(CO)_6$ is based on an estimated log *A* value for the pre-exponential factor *A* in the Arrhenius equation. The observed log *A* value was considered to be too large and a value obtained from studies on $Mo(CO)_6$, $W(CO)_6$, and $Fe(CO)_5$ was adopted instead. Nevertheless, if the measured log *A* value is used for the estimate of ΔH^{298}, the corresponding FBDE would be about 47 kcal/mol, in better agreement with the CCSD(T) and NL-SCF+QR results, Table 8. It would seem that no clear consensus has been reached yet as to the order of the FBDE's within the hexacarbonyls of the chromium triad. We shall in the following analyze some of the kinetic data that might shed further light on this subject with the aid of supplementary calculations on the $M(CO)_7$ systems.

Table 7. Calculated and Experimental M−C and C−O Bond Lengths (Å) for $M(CO)_6$

	$Cr(CO)_6$		$Mo(CO)_6$		$W(CO)_6$	
method	M−C	C−O	M−C	C−O	M−C	C−O
LDA	1.866	1.145	2.035	1.144	2.060	1.144
NL-SCF	1.910	1.153	2.077	1.152	2.116	1.154
NL-SCF+QR	1.910	1.153	2.076	1.153	2.049	1.155
MP2[a]	1.883	1.168	2.066	1.164	2.054	1.166
CCSD(T)[b]	1.939	1.178				
exp[c]	1.918	1.141	2.063	1.145	2.058	1.148

[a] Reference 26. [b] Reference 49. [c] Reference 48.

Table 8. First Bond Dissociation Energies, FBDE's, of $M(CO)_6$ and the Association Energies, AE's, for $M(CO)_6$ + CO

	FBDE (kcal/mol)			AE (kcal/mol)		
method[a]	$Cr(CO)_6$	$Mo(CO)_6$	$W(CO)_6$	$Cr(CO)_6$	$Mo(CO)_6$	$W(CO)_6$
LDA	62.1	52.7	48.4	49.7	39.7	37.3
LDA/NL	44.6	37.4	33.5	46.3	40.3	32.1
LDA/NL+FO	45.1	39.8	41.8	46.8	42.2	43.3
NL-SCF	45.9	38.2	38.8			
NL-SCF/FO	46.8	40.6	47.2			
NL-SCF+QR	46.2	39.7	43.7	47.0	40.4	35.8
MP2[b]	20.3	28.4	37.7	19.1	27.3	35.8
MP2[c]	58.0	46.1	54.9			
CCSD(T)[c]	45.8	40.4	48.0			
CCSD(T)[d]	42.7					
exp[e]	36.8 ± 2	40.5 ± 2	46.0 ± 2			
exp[f]	40.2	31.7	39.9			
exp[g]	38.7	30.1	39.7			

[a] See footnote *a* of Table 2. [b] Reference 51a. [c] Reference 26. [d] Reference 49. [e] Accurate gas-phase values based on pulsed laser pyrolysis, ref 4. [f] Estimate based on the activation energy for the dissociation path in the CO substitution process of eq 4 with L = P(*n*-$C_4H_9)_3$, ref 51c. [g] Estimate based on the activation energy for the CO exchange process of eq 4 with L = CO, ref 2a.

Experimental investigations have shown that the substitution reaction[2,50]

$$M(CO)_6 + L \rightarrow M(CO)_5L + CO \quad (4)$$

has a kinetics consistent with the rate constant expression

$$\text{rate} = (k_1 + k_2[L])[M(CO)_6] \quad (5)$$

for M = Cr, Mo, and W. The constant k_1 is interpreted as the rate constant for a dissociative mechanism (D) in which the rate-determining step is represented by CO dissociation

$$M(CO)_6 \rightarrow M(CO)_5 + CO \quad (6)$$

followed by the fast capture of the ligand L by $M(CO)_5$. The constant k_2 represents on the other hand an associative pathway

$$M(CO)_5 + L \longrightarrow \begin{matrix} L \\ \diagdown \\ M(CO)_5 \\ \diagup \\ OC \end{matrix} \longrightarrow M(CO)_5L + CO \quad (7)$$

(46) Atwood, J. D. *Inorganic and Organometallic Reaction Mechanisms*; Brooks/Cole: Monterey, CA, 1985.
(47) Li, J.; Schreckenbach, G.; Ziegler, T. *J. Phys. Chem.* **1994**, in press.
(48) Jost, A.; Rees, B. *Acta Crystallogr.* **1975**, *B31*, 2649.
(49) Barnes, L. A.; Liu, B.; Lindh, R. *J. Chem. Phys.* **1993**, *98*, 3978.
(50) Wieland, S.; van Eldik, R. *Organometallics* **1991**, *10*, 3110.

in which at least some M−L bond formation takes place before the M−CO bond of the departing carbonyl ligand is completely broken.[51b]

The activation energies, $\Delta H_1^{\#}$, for the dissociative path have been measured[2a,51c] in the case of L = P(n-C_4H_9)$_3$ as 40.2 (Cr), 31.7 (Mo), and 39.9 (W) kcal/mol. The activation energy, $\Delta H_1^{\#}$, should be closely related to the FBDE's for the M(CO)$_6$ systems, and we note that our calculated FBDE's in fact follow the same order of Cr ~ W > Mo as the observed activation energies, $\Delta H_1^{\#}$, Table 8. Activation energies, $\Delta H_{ex}^{\#}$, for the CO exchange reaction with L = CO in eq 4 have been measured as 38.7 (Cr), 30.2 (Mo), and 39.8 (W) kcal/mol. This trend establishes again the 4d member of a triad as having the most labile M−L bond, a trend also observed for the nickel[51b] and iron[45a] triads.

The activation energy for the CO exchange process, $\Delta H_{ex}^{\#}$, represents the overall reaction. It is not clear whether it corresponds to a dissociative or associative path, or even the same path for all three members of the chromium triad. We have in order to examine this point extended our study to the M(CO)$_7$ systems (M = Cr, Mo, and W), where M(CO)$_7$ would serve as a model for the transition state of the associative path in the CO exchange reaction.

According to the principle of microscopic reversibility the associative transition state M(CO)$_7$ should possess identical entering and leaving CO ligands. The entering CO ligand may attack either from the edge or face of the octahedral M(CO)$_6$ complex. Lin and Hall found from calculations based on Hartree−Fock optimized geometries of several possible structures[51] that the M(CO)$_7$ conformation corresponding to the face-attacking mode is lowest in energy. This mode of attack was also suggested by Therien and Trogler from an orbital analysis.[52] We thus adopt the configuration of M(CO)$_7$, **3**, as suggested from these studies, and optimized the geometries within C_{2v} symmetry constraint. The optimized parameters are shown in Table 9. The energy of formation of M(CO)$_7$ from M(CO)$_6$ and CO is shown to the right in Table 8 as AE (association energy). A positive value indicates that M(CO)$_7$ is of higher energy than the sum of the energies for the separate M(CO)$_6$ and CO fragments.

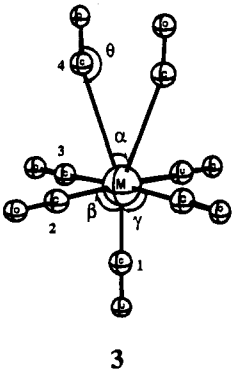

3

It is clear from Table 9 that **3** consists of a M(CO)$_5$ core and two weakly associated CO ligands. The M(CO)$_5$ core has nearly the same structure as the free pentacarbonyl fragments[47] of the chromium triad, with one shorter M−CO_{ax} distance and four longer M−CO_{eq} bonds. The distance from the metal center to the two loosely associated CO ligands is 1.2 Å longer than a regular M−CO bond length according to the NL-SCF+QR scheme. The distance is even longer, by 1 Å, in the *ab initio* Hartree−Fock picture, Table 9. The CO−M−CO angle, α, involving the entering and leaving CO ligands is in the range of 50° to 60° for both HF and NL-SCF+QR. The weakly associated CO ligands form a bent M−CO bond with a bending angle θ, **3**, that is 158°, 172°, and 156° for Cr, Mo, and, W, respectively, in the NL-SCF+QR picture. We observe that the molybdenum system differs somewhat from its chromium and tungsten congeners in having the longest M−C_4 distance and smallest θ angle.

Table 9. Optimized Geometries of M(CO)$_7$ at the NL-SCF+QR Level[a]

	Cr(CO)$_7$	Mo(CO)$_7$	W(CO)$_7$
M−C_1	1.852	1.996	1.915
M−C_2	1.916	2.096	2.050
M−C_3	1.917	2.095	2.039
M−C_4	3.122 (4.23)[b]	3.267 (4.23)[b]	3.120 (3.91)[b]
C_1−O	1.165	1.158	1.175
C_2−O	1.158	1.151	1.162
C_3−O	1.160	1.151	1.162
C_4−O	1.139	1.133	1.138
α	55.0 (62.5)[b]	50.0 (60.0)[b]	54.0 (57.4)[b]
β	89.8	89.8	89.8
γ	87.2	89.5	87.6
θ	158.2	172.3	156.0

[a] Bond lengths in angstroms and bond angles in degrees. [b] Data in parentheses are HF results, ref 51.

Structure **3** represents a system in which very little bond making has taken place between the entering group and the metal center and where very little is left of the bond between the leaving ligand and the metal. Thus, **3** is consistent with an associative I_d mechanism and only to a small degree different from a dissociative transition state. It would appear that the distinction between a dissociative and an associative path is very fine for the CO exchange reaction.

The association energies, AE's, obtained at the NL-SCF+QR level, 47.0 (Cr), 40.4 (Mo), and 41.1 (W) kcal/mol, are very close to the corresponding FBDE's, 46.2 (Cr), 39.7 (Mo), and 43.7 (W) kcal/mol. This was also found to be the case in the HF calculations, although the absolute values by this method are believed to be too small. We note that the NL-SCF+QR method finds the molybdenum system to have the smallest value for both FBDE and AE. Thus, our calculations point to the Mo−CO bond as being the most labile irrespective of whether the CO exchange reaction goes by a D or I_d mechanism. We calculate the difference, FBDE − AE, for the three compounds in the triad as −0.8, −0.7, and +2.6 kcal/mol for Cr, Mo, and W compounds, respectively. These numbers are consistent with a gradual changeover from a more dissociative to a more associative process along the Cr, Mo, and W triad. However, the distinction between D and I_d seems to be quite fine for the CO exchange process.

e. Relativistic Effects. It is well-known that relativistic effects influence the properties of heavier elements in a number of ways.[53] We have in the present investigation studied the impact of relativity on the M−CO bond energies and bond lengths among binary metal carbonyls and summarize in the following our findings.

(51) (a) Lin, Z.; Hall, M. B. *Inorg. Chem.* **1992**, *31*, 2791. (b) Jordan, R. B. *Reaction Mechanisms of Inorganic and Organometallic Reaction Mechanisms*; Oxford University Press: Oxford, 1991. (c) Day, J. P.; Basolo, F.; Pearson, R. G. *J. Am. Chem. Soc.* **1968**, *90*, 6927.

(52) Therien, M. J.; Trogler, W. C. *J. Am. Chem. Soc.* **1988**, *110*, 4942.

(53) (a) Pyykkö, P.; Declaux, J.-P. *Acc. Chem. Res.* **1979**, *12*, 276. (b) Pyykkö, P. *Chem. Rev.* **1988**, *88*, 563. (c) Ziegler, T.; Snijders, G. J.; Baerends, E. J. In *The challenge of d and f electrons, Theory and computation; ACS Symposium Series 349*, Salahub, D. R., Zerner, M. C., Eds.; American Chemical Society: Washington, DC, 1989. (d) Schwarz, W. H. E.; van Wezenbeek, E. M.; Baerends, E. J.; Snijders, G. J. *J. Phys. B* **1989**, *22*, 1515.

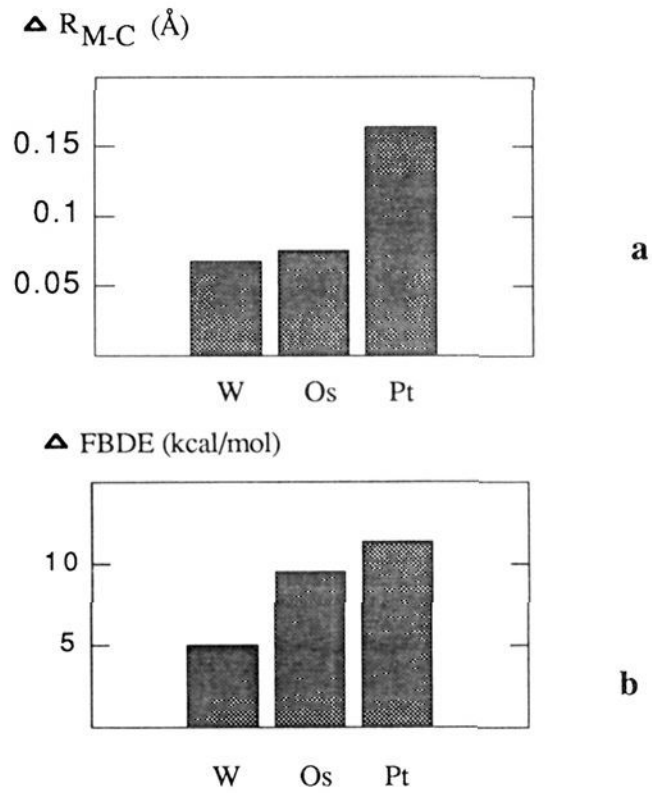

Figure 1. Relativistic effects on M−CO bond lengths (a) and first bond dissociation energies (b) for $W(CO)_6$, $Os(CO)_5$, and $Pt(CO)_4$.

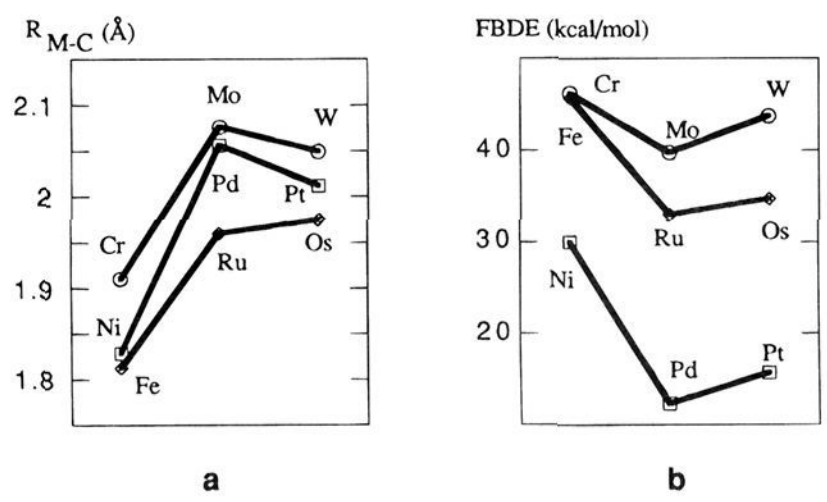

Figure 2. Calculated M−CO bond lengths (a) and first bond dissociation energies (b) at the NL-SCF+QR level for $M(CO)_4$ (M = Ni, Pd, Pt), $M(CO)_5$ (M = Fe, Ru, Os), and $M(CO)_6$ (M = Cr, Mo, W).

Figure 1a outlines the relativistic M−CO bond contractions. They are substantial for the 5d elements, amounting to 0.07, 0.08, and 0.16 Å for M = W, Os, and Pt, respectively, and much more modest for the 4d series with values of 0.01, 0.02, and 0.03 Å for M = Mo, Ru, and Pd, whereas the contraction among 3d elements is negligible. Without the relativistic bond contraction, the M−CO bond length would increase monotonously from first row to third row along the triads. The relativistic bond contraction results on the other hand in a maximum for the M−CO bond lengths of the second-row elements in the Cr and Ni triads, Figure 2a. The origin of the relativistic bond contraction has been analyzed elsewhere. It is mainly due to a reduction in the electronic kinetic energy caused by the mass-velocity correction.[54]

The extent to which relativity increases the M−CO bond energies is summarized in Figure 1b. There is a substantial increase in the FBDE's of the 5d elements by 5.0, 9.5, and 11.3 kcal/mol, respectively, for $W(CO)_6$, $Os(CO)_5$, and $Pt(CO)_4$. The increase among the 4d elements is by comparison modest with values of 1.5, 3.3, and 1.4 kcal/mol respectively for $Mo(CO)_6$, $Ru(CO)_5$, and $Pd(CO)_4$. At the nonrelativistic LDA or NL-SCF levels, the FBDE's decrease monotonously from first row to third row in every triad. This trend changes when relativistic effects are taken into account. At the NL-SCF+QR level, the FBDE's show a shallow minimum for the second-row compounds, Figure 2b, for all three triads. We note finally that the relativistic impact on M−CO bond energies and bond distances increases from left to right within a transition series.

(54) (a) Ziegler, T.; Snijders, G. J.; Baerends, E. J. *Chem. Phys. Lett.* **1980**, *75*, 1. (b) Ziegler, T.; Snijders, G. J.; Baerends, E. J.; Ros, P. *J. Chem. Phys.* **1981**, *74*, 1271.

Table 10. Decomposition of FBDE (kcal/mol) for $Pt(CO)_4$, $Os(CO)_5$, and $W(CO)_6$ at the Nonrelativistic NL-SCF (NR) and Relativistic NL-SCF+QR (R) Levels[a]

		E_{steric}	$E(a_1)$	$E(e)^b$	$E_{orb}{}^c$	E_{prep}	FBDE
$Pt(CO)_4$	NR	51.6	−25.5	−31.0	−56.5	2.8	2.1
	R	47.7	−30.7	−35.6	−66.3	2.9	15.7
$Os(CO)_5$	NR	69.5	−54.5	−42.5	−97.0	4.0	23.5
	R	65.3	−37.3	−67.2	−104.5	4.5	34.7
$W(CO)_6$	NR	39.5	−29.2	−44.2	−73.4	0.3	34.2
	R	35.0	−19.6	−60.1	−79.7	1.0	43.7

[a] The geomtries used in the ETS calculations, NR as well as R, are those obtained at the NL-SCF+QR level. [b] For $Os(CO)_5$, $E(b_1 + b_2)$. [c] $E_{orb} = E(a_1) + E(e)$.

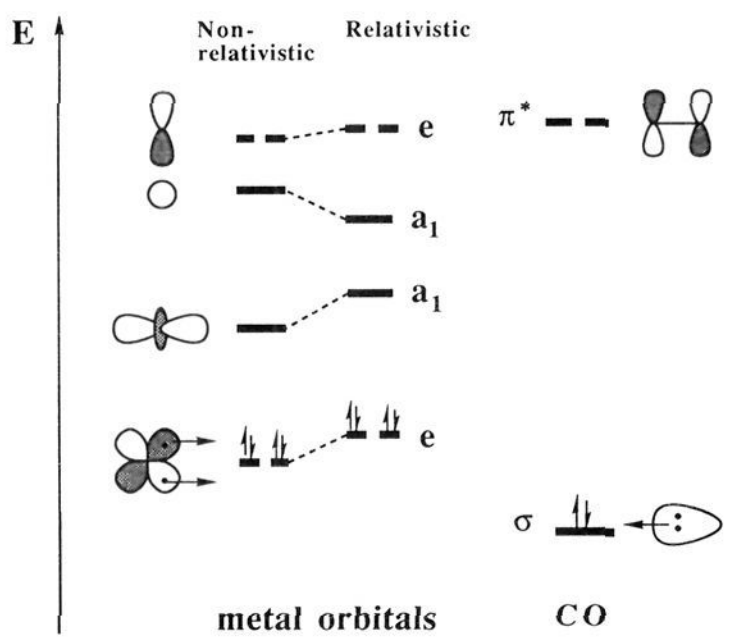

Figure 3. The influences of relativistic effects on metal−carbonyl donation and back-donation in M−CO bonding.

It might be instructive to carry out an analysis based on the extended transition state (ETS) method[27] in order to understand how relativistic effects influence the M−CO bond strengths. Table 10 displays an ETS decomposition of the FBDE's for the three third-row metal carbonyls according to eq 2 at the NL-SCF and NL-SCF+QR levels of theory. For $Os(CO)_5$, we only consider the case where an equatorial CO ligand is removed. The point groups preserved during the formation of $Os(CO)_5$, $Pt(CO)_4$, and $W(CO)_6$ are C_{2v}, C_{3v}, and C_{4v}, respectively. Therefore, the contribution from the a_1 representation, $E(a_1)$, represents the σ_{C-O} to metal donation interaction while the contributions from the e representation (C_{3v} and C_{4v} groups) or b_1 and b_2 representations (C_{2v} group), $E(e)$ or $E(b_1+b_2)$, are due to the d_π to π_{C-O}* back-donation interaction.

As can be seen from Table 10, relativistic effects increase the contribution to the bond energy from the d_π to π_{C-O}* back-donation interaction, $E(e)$ or $E(b_1+b_2)$, for $Pt(CO)_4$, $Os(CO)_5$, and $W(CO)_6$. This trend is understandable in considering the general relativistic destabilization[53d] of 5d orbitals for third-row atoms. The higher energy of d_π will reduce the $d_\pi-\pi_{C-O}$* gap and thus enhance the back-donation interaction as illustrated in Figure 3. The effect is smallest in $Pt(CO)_4$ where the d-levels are lowest in energy compared to π_{C-O}*. Since the back-donation interaction is the dominant stabilizing contribution to the M−CO bond energies, relativity increases in all cases the FBDE's.

The contribution from the σ_{C-O} to metal donation interaction $E(a_1)$ is reduced by relativity in the cases of M = W and Os

since the donation is to $5d_\sigma$(W) and $6p_\sigma$(Os) based orbitals, both of which are raised in energy by relativity,[53d] Figure 3. In the case of $Pt(CO)_4$, the donation is to a metal based orbital with an appreciable 6s contribution, and $-E(a_1)$ is increased by relativity due to the relativistic stabilization[53d] of 6s, Figure 3.

IV. Conclusion

We have demonstrated that the DFT based techniques at the NL-SCF+QR level with nonlocal corrections and relativistic effects included self-consistently can provide a good fit to experimental M−CO bond distances and first bond dissociation energies for the homologous series of tetra-, penta-, and hexacarbonyls. The deviations between calculated and observed M−CO bond lengths and FBDE's are usually within 0.01 Å and 5 kcal/mol, respectively. Thus, the NL-SCF+QR scheme affords estimates with the same accuracy as the highly correlated CCSD(T)[26] and MCPF *ab initio* techniques. The present investigation constitutes a substantial improvement over a previous DFT study[8] on the same series of compounds by including nonlocal and relativistic effects self-consistently and performing full geometry optimizations on all species. The more accurate calculations presented in the present paper support the main conclusion reached in the previous DFT study,[8] namely that the M−CO bonds of the 4d elements are the most labile within a triad of homologous carbonyls. It should be pointed out that results of the same quality as those presented here can be obtained by the CCSD(T) *ab initio* method.[26]

Relativistic effects are found to be essential for an accurate representation of the M−CO bond lengths and M−CO bond energies, especially for third-row compounds. Relativity contracts M−CO bonds by 0.07−0.16 Å and increases FBDE's by 5−11 kcal/mol in the case of the tungsten, osmium, and platinum carbonyls. As a result, we find the M−CO bond of the 4d member within a triad to be the weakest and most labile. It is shown that our findings are in-line with kinetic observation. The way in which relativistic effects increase the M−CO bond strength is analyzed by the ETS energy decomposition scheme. It is shown that relativity increases the metal to ligand back-donation by raising the energy of the d-levels.

Acknowledgment. This investigation was supported by the Natural Sciences and Engineering Research Council of Canada (NSERC) as well as the donors of the Petroleum Research Fund, administered by the American Chemical Society (ACS-PRF NO. 27023-AC3). J.L. thanks NSERC for an International Research Fellowship, and G.S. acknowledges a scholarship from the department of chemistry. The University of Calgary is acknowledged for access to the IBM-6000/RISC facilities.

JA941168L